

## Characterization of Tritium Isotopic Permeation Through ARAA in Diffusion Limited and Surface Limited Regimes

Hongjie Zhang, Alice Ying, Mohamed Abdou, Masashi Shimada, Bob Pawelko & Seungyon Cho

To cite this article: Hongjie Zhang, Alice Ying, Mohamed Abdou, Masashi Shimada, Bob Pawelko & Seungyon Cho (2017) Characterization of Tritium Isotopic Permeation Through ARAA in Diffusion Limited and Surface Limited Regimes, *Fusion Science and Technology*, 72:3, 416-425, DOI: [10.1080/15361055.2017.1333826](https://doi.org/10.1080/15361055.2017.1333826)

To link to this article: <https://doi.org/10.1080/15361055.2017.1333826>



Published online: 22 Jun 2017.



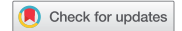
Submit your article to this journal [↗](#)



Article views: 52



View Crossmark data [↗](#)



# Characterization of Tritium Isotopic Permeation Through ARAA in Diffusion Limited and Surface Limited Regimes

Hongjie Zhang,<sup>a\*</sup> Alice Ying,<sup>a</sup> Mohamed Abdou,<sup>a</sup> Masashi Shimada,<sup>b</sup> Bob Pawelko,<sup>b</sup> and Seungyon Cho<sup>c</sup>

<sup>a</sup>UCLA, Mechanical and Aerospace Engineering Department, Los Angeles, California

<sup>b</sup>Idaho National Laboratory, Idaho Falls, Idaho

<sup>c</sup>ITER Korea National Fusion Research Institute, Daejeon, Korea

Received September 13, 2016

Accepted for Publication February 28, 2017

**Abstract** — A mathematical model for permeation of multi-components ( $H_2$ ,  $T_2$ , HT) through a RAFM (Reduced activation ferritic/martensitic) membrane was described based on kinetic theory. Experimental conditions of tritium permeation for ARAA (Advanced Reduced Activation Alloy) material performed at INL were recreated in simulations for model validation. Both numerical simulations and experimental data indicated that the presence of hydrogen reduces tritium permeation rate significantly in low tritium partial pressure with 1000 ppm (0.1%) hydrogen-helium gas mixture at 1atm. Experimental behavior of tritium permeation flux dependence on tritium isotope partial pressure confirmed the kinetic theory. i.e., it still follows diffusion-controlled, square root dependence, with  $T_2$  partial pressures and a linear dependence HT pressure even though it is in a diffusion-controlled regime. In addition, the numerical model was validated with literature data for mono-isotope permeation through oxidized and clean MANET II (MArtensitic for NET) samples under surface-controlled and diffusion-controlled regimes. The simulation results agreed well with the experimental data, which indicated that the mono permeation rate through the oxidized sample is much lower (~2 orders) than clean sample and the permeation rate is proportional to  $p^1$  and  $p^{0.5}$  for oxidized and clean MANET II samples, respectively.

**Keywords** — Tritium, isotope permeation, permeability.

**Note** — Some figures may be in color only in the electronic version.

## I. INTRODUCTION

To develop a multi-physics dynamic predictive tool for computational simulation of tritium transport in fusion blanket systems, there is a need to develop a multi-component ( $H_2$ ,  $T_2$ , HT) permeation model to accurately predict tritium transport and permeation behavior at realistic TBS (Test Blanket System) tritium conditions.<sup>1</sup> Meanwhile, relevant experiments are necessary to provide data for model validations and to better understand tritium co-permeation behavior through a RAFM material (ARAA, F82H, MANET II, etc.).

Table I gives the compositions of these RAFM steels. They are still undergoing development and characterization from the point of view of their mechanical, physical and tritium permeation properties. Tritium permeation through a RAFM material is typically investigated at high pressure (>1000 Pa) with mono-isotope permeation (hydrogen or deuterium). However, in a typical ITER TBS, e.g. HCCR (Helium Cooled Ceramic Reflector) TBS (Ref. 2), the tritium partial pressure in the purge gas is expected to be low (~0.16 Pa or less than 1 Pa). There have been concerns that tritium permeation behavior may not follow the diffusion-controlled mechanism at low tritium partial pressure.<sup>3</sup> Also, the presence of high pressure hydrogen in the purge gas may affect the

\*E-mail: [zhjbook@gmail.com](mailto:zhjbook@gmail.com)

TABLE I

Main Chemical Composition of RAFM Materials Referenced in This Study (wt%)

	ARAA	MANET II	F82H
C	0.08–0.12	0.11	0.09
Si	0.05–0.15	0.18	0.13
Mn	0.3–0.6	0.85	0.18
Cr	8.7–9.3	10.3	7.8
W	1.0–1.4	–	2
V	0.05–0.3	0.19	0.16
Ta	0.005–0.09	–	0.02
N	0.005–0.015	0.03	0.006
B	<0.002	0.0072	<0.001
Ti	0.005–0.02	–	<0.02
Zr	0.005–0.02	0.014	–
Mo	<0.005	0.58	<0.01
S	<0.005	0.004	0.003
P	<0.005	0.005	0.004

permeation behavior.<sup>4</sup> In addition, oxidized or contaminated surfaces tend to increase the importance of the surface effects, tritium permeation could be completely controlled by the surface processes.<sup>5</sup> Improved understanding of tritium permeation behavior is crucial to minimize the uncertainty associated with model predication of tritium permeation at realistic TBS tritium conditions: 1) low tritium partial pressure, usually less than 1 Pa; 2) hydrogen effects,  $p_{H_2} \sim 100$  Pa; 3) surface effects, e.g., oxidized or clean surface. Therefore, the objective of this research is to: 1) develop a mathematical model for tritium permeation of a multi-component ( $H_2$ ,  $T_2$ , HT) system; 2) identify expected tritium permeation through ARAA dominated by either surface or diffusion controlled regime; and 3) validate the numerical model with experimental data and literature data at realistic TBS tritium conditions.

Within the collaborative study with Korea NFRI (National Fusion Research Institute), tritium permeation properties are being measured for Korea's ARAA as the material using the TGAP (Tritium Gas Absorption Permeation) experiments at the STAR (Safety and Tritium Applied Research) facility at INL. A series of multi-components tritium permeation modeling efforts were performed by UCLA including pre-analysis to assist INL ARAA permeation experimental designs, and post-analysis to interpret and validate against literature data and ARAA experimental data. In this paper we first give a model description of co-permeation of H and T in a multi-component ( $H_2$ ,  $T_2$  and HT) system; then we compare the experimental observations and literature data with the model simulations.

## II. THEORY

A simple schematic of tritium permeation model in a multi-component ( $H_2$ ,  $T_2$  and HT) system was shown in Fig. 1. The symbols  $p_{H_2}$ ,  $p_{HT}$ , and  $p_{T_2}$  are respectively partial pressures of  $H_2$ , HT and  $T_2$  in the gas phase. The symbols  $c_H$  and  $c_T$  are respectively the concentrations of H and T in the solid just below the gas-metal interface.

It is well known that under certain conditions (i.e., low pressure level, oxidized or contaminated surfaces, multi-components, etc.) the tritium permeation behavior could be in either surfaced-controlled or diffusion-controlled regimes. For better understanding of tritium permeation behavior, it would be necessary to apply classical kinetic theory at the surface in a multi-component ( $H_2$ ,  $T_2$ , HT) system.

If two isotopes, hydrogen H and tritium T, co-exist in a metal solid, they may desorb from the surface as  $H_2$ ,  $T_2$ , and HT molecules. The respective molecules desorption fluxes ( $mol\ m^{-2}\ s^{-1}$ ) are:

$$J_{H_2} = (\sigma k_{2\_HH}) c_H^2, \quad (1)$$

$$J_{T_2} = (\sigma k_{2\_TT}) c_T^2, \quad (2)$$

$$J_{HT} = (2\sigma k_{2\_HT}) c_H c_T, \quad (3)$$

where  $k_{2\_HH}$ ,  $k_{2\_TT}$  and  $k_{2\_HT}$  are known as recombination constants ( $mol^{-1}\ m^4\ s^{-1}$ ) for  $H_2$ ,  $T_2$  and HT, and  $\sigma$  is the surface roughness factor, defined as the ratio of the real area to the geometric area of the surface.<sup>3</sup>

The release fluxes of H and T atoms in  $H_2$ ,  $T_2$  and HT molecules are

$$j_{H\_H_2} = 2J_{H_2} = 2(\sigma k_{2\_HH}) c_H^2, \quad (4)$$

$$j_{H\_HT} = J_{HT} = 2(\sigma k_{2\_HT}) c_H c_T, \quad (5)$$

$$j_H = j_{H\_H_2} + j_{H\_HT}, \quad (6)$$

and

$$j_{T\_T_2} = 2J_{T_2} = 2(\sigma k_{2\_TT}) c_T^2, \quad (7)$$

$$j_{T\_HT} = J_{HT} = 2(\sigma k_{2\_HT}) c_H c_T, \quad (8)$$

$$j_T = j_{T\_T_2} + j_{T\_HT}. \quad (9)$$

The fluxes of  $H_2$ ,  $T_2$ , and HT molecules that dissociate on the surface are

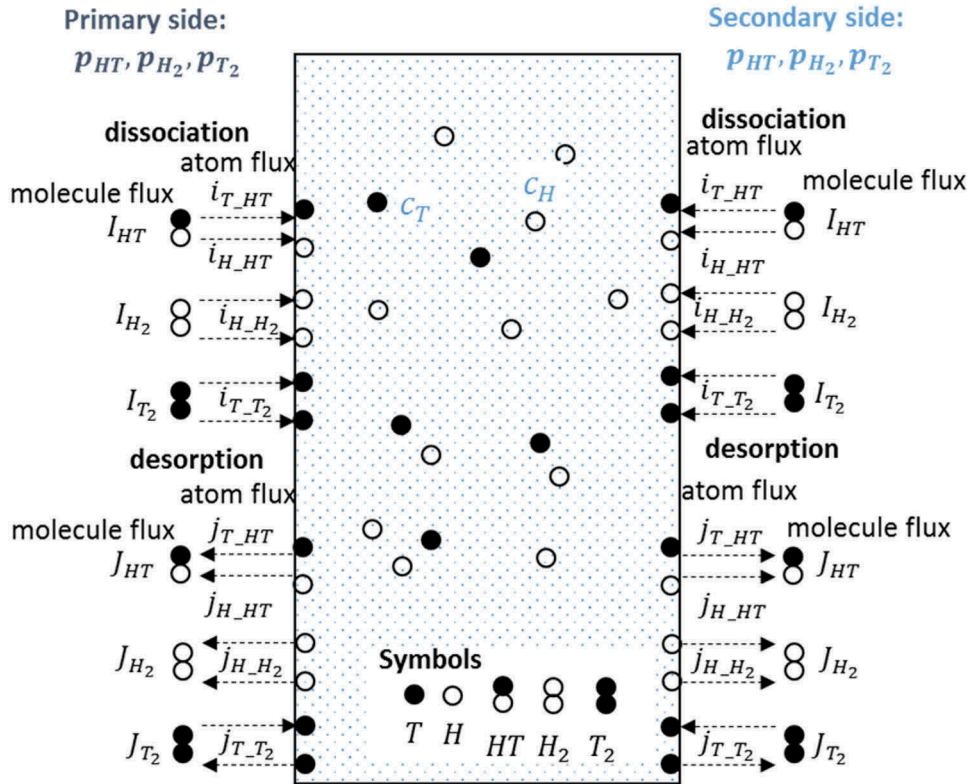


Fig. 1. Isotope permeation model in a multi-component (H<sub>2</sub>, T<sub>2</sub> and HT) system.

$$I_{H_2} = (\sigma k_{1\_HH}) p_{H_2} , \quad (10)$$

$$I_{T_2} = (\sigma k_{1\_TT}) p_{T_2} , \quad (11)$$

$$I_{HT} = (\sigma k_{1\_HT}) p_{HT} , \quad (12)$$

where  $k_{1\_HH}, k_{1\_TT}$  and  $k_{1\_HT}$  are known as the adsorption constants ( $mol\ m^{-2}\ s^{-1}\ Pa^{-1}$ ) for H<sub>2</sub>, T<sub>2</sub> and HT. The incident adsorbed fluxes of H and T atoms due to dissociation of H<sub>2</sub>, T<sub>2</sub>, and HT molecules on the surface are

$$i_{H\_H_2} = 2(\sigma k_{1\_HH}) p_{H_2} , \quad (13)$$

$$i_{T\_T_2} = 2(\sigma k_{1\_TT}) p_{T_2} , \quad (14)$$

$$i_{H\_HT} = i_{T\_HT} = (\sigma k_{1\_HT}) p_{HT} . \quad (15)$$

The net fluxes of H and T atoms into the surface are, respectively,

$$j_{T\_net} = 2\sigma k_1 \left( p_{T_2} + \frac{1}{2} p_{HT} \right) - 2\sigma k_2 c_T (c_H + c_T) , \quad (17)$$

$$j_{H\_net} = 2\sigma k_1 \left( p_{H_2} + \frac{1}{2} p_{HT} \right) - 2\sigma k_2 c_H (c_H + c_T) . \quad (18)$$

If the tritium permeation behavior is under a surface-controlled regime, i.e., governed by the physical-chemical reactions (adsorption, desorption) occurring at the surface of the material, the surface-controlled processes can be evaluated by the H and T atoms net fluxes entering the material expressed in Eqs. (17) and (18).

When the multi-component (H<sub>2</sub>, T<sub>2</sub>, HT) system is under an equilibrium state at the surface and in gas phase, two kinds of equilibriums are established: 1) Gas phase equilibrium between H<sub>2</sub>, T<sub>2</sub> and HT and 2) Surface equilibrium between H<sub>2</sub>/T<sub>2</sub>/HT molecules and dissolved H/T atoms (denoted as H\* and T\*) as shown:



Under equilibrium condition, the balances of atomic fluxes at the surface are

$$i_{H-H_2} + i_{H-HT} = j_{H-H_2} + j_{H-HT}, \quad (23)$$

$$i_{T-T_2} + i_{T-HT} = j_{T-T_2} + j_{T-HT}, \quad (24)$$

which gives

$$\begin{aligned} & 2(\sigma k_{1-HH})p_{H_2} + 2(\sigma k_{1-TT})p_{T_2} + 2(\sigma k_{1-HT})p_{HT} \\ & = 2(\sigma k_{2-HH})c_H^2 + 2(\sigma k_{2-TT})c_T^2 + 4(\sigma k_{2-HT})c_H c_T. \end{aligned} \quad (25)$$

From this equation, the partial balances in this equilibrium are

$$(\sigma k_{1-HH})p_{H_2} = (\sigma k_{2-HH})c_H^2, \quad (26)$$

$$(\sigma k_{1-TT})p_{T_2} = (\sigma k_{2-TT})c_T^2, \quad (27)$$

$$(\sigma k_{1-HT})p_{HT} = 2(\sigma k_{2-HT})c_H c_T. \quad (28)$$

The concentrations of H and T atoms on metal surface at equilibrium expressed as

$$c_H = \sqrt{(\sigma k_{1-HH})/(\sigma k_{2-HH})p_{H_2}} = K_{s-H}\sqrt{p_{H_2}}, \quad (29)$$

$$c_T = \sqrt{(\sigma k_{1-TT})/(\sigma k_{2-TT})p_{T_2}} = K_{s-T}\sqrt{p_{T_2}}. \quad (30)$$

Equation (28) gives that the HT pressure in the gas mixture at equilibrium can be expressed with the concentrations at solid surface in the equilibrium:

$$p_{HT} = \sqrt{\frac{4(\sigma k_{2-HT})^2(\sigma k_{1-HH})(\sigma k_{1-TT})}{(\sigma k_{1-HT})^2(\sigma k_{2-HH})(\sigma k_{2-TT})}} p_{H_2} p_{T_2}. \quad (31)$$

The gas phase equilibrium constant ( $K_{HT}$ ) can be obtained from the gas phase equilibrium [Eq. (19)] as

$$K_{eq} = \frac{p_{HT}^2}{p_{H_2} p_{T_2}}. \quad (32)$$

Combining Eqs. (31) and (32) gives

$$K_{eq} = \frac{4(\sigma k_{2-HT})^2(\sigma k_{1-HH})(\sigma k_{1-TT})}{(\sigma k_{1-HT})^2(\sigma k_{2-HH})(\sigma k_{2-TT})}. \quad (33)$$

Tritium atom concentrations on a metal surface at equilibrium is given as

$$c_T = K_{s-T}\sqrt{p_{T_2}} = \frac{K_{s-T}}{\sqrt{K_{eq}p_{H_2}}}p_{HT} \quad (34)$$

where the equilibrium constant is expressed as<sup>5</sup>

$$K_{eq} = 4.662K_0 \exp\left(-\frac{176.3}{T}\right) \quad (35)$$

$$\text{where } K_0 = \frac{(1 - \exp(-5986/T))(1 - \exp(-3548/T))}{(1 - \exp(-4940/T))^2}.$$

From Eq. (34), we can see that the equilibrium concentrations of T atoms on a metal surface remain as a square root dependence with  $T_2$  partial pressure. Meanwhile, tritium equilibrium concentration is also linearly dependent on the partial pressure of HT and inversely proportional to the square root of partial pressure of  $H_2$ . Under realistic blanket tritium gas stream conditions where  $p_{H_2} \gg p_{HT} \gg p_{T_2}$ , the tritium equilibrium concentrations can be stated as a linear dependence on HT pressure. Equation (34) also indicates that tritium permeation flux is significantly reduced by the presence of hydrogen. As shown in Fig. 2, the tritium permeation reduction is up to 2 orders when the driving pressure  $p_{HT}$  is 0.01 Pa and  $H_2$  pressure is at 100 Pa.

It is worth noting that the theory and equations described in this section are also applied to mono-isotope permeation. If  $H_2$  pressure is zero, the surface atom net flux equations [Eqs. (17) and (18)] and tritium equilibrium concentrations [Eq. (34)] are reduced to single component equations.<sup>6</sup>

For practical purpose, based on E. Serra's theory,<sup>6</sup> the permeation flux is a linear dependence on driving pressure if permeation is surface limited. Considering the H/T

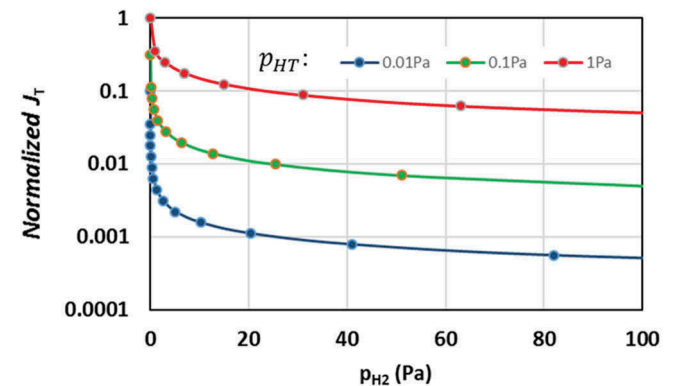


Fig. 2. Tritium equilibrium concentrations on metal surface are reduced by the presence of hydrogen in the gas.

co-permeation case, the total permeation flux of H and T atoms  $j$  can be written as

$$j = j_T + j_H = \sigma k_1 (p_{T_2} + p_{HT} + p_{T_2}) . \quad (36)$$

Then the T atom flux can be expressed as

$$j_T = x_T \sigma k_1 (p_{T_2} + p_{HT} + p_{T_2}) , \quad (37)$$

where  $x_T = \frac{p_{T_2} + \frac{1}{2}p_{HT}}{p_{T_2} + p_{HT} + p_{T_2}}$  is the atomic fractions of T in the gas phase. Then Eq. (37) is reduced to

$$j_T = \sigma k_1 \left( p_{T_2} + \frac{1}{2}p_{HT} \right) . \quad (38)$$

If equilibrium conditions in gas phase and at the surface are not established, Eq. (38) indicates that the tritium permeation flux doesn't follow a square root dependence of  $T_2$  partial pressure.

### III. EXPERIMENTS AND MODEL

#### III.A. Experimental Setup

Tritium permeation experiments for KO Advanced Reduced Activation Alloy (ARAA) material were conducted at the TGAP facility at INL.

The principle set-up at INL for the permeation experiment shown in Fig. 3 involves placing the ARAA sample between the two dynamic flowing gas chambers (defined as the primary flowing system – the upstream and the secondary flowing system – the downstream). The gas is delivered to the sample through a 1/8-inch inlet pipe and returns through a 1/4-inch pipe. The arriving hydrogen isotopes (tritium/hydrogen or deuterium) dissolve at the sample

surface into two atoms while they diffuse through the sample, recombine into molecules at the other side of the surface, leave the sample, and are collected by the secondary gas system to a tritium measuring system.

There are two ion chambers measuring tritium concentrations at both return lines of the primary (pIC) and the secondary (sIC) flow lines. The tritium source side (primary) gas supply system is designed to be able to control the  $H_2$  and  $T_2$  concentrations, and the sweep (secondary) gas supply system is designed to be able to capture higher HT throughput. The ranges of experimental conditions are listed in Table II.

#### III.B. Numerical Model

The general form of the tritium isotope mass transport equation can be written as

$$\frac{\partial c_i}{\partial t} + \nabla \cdot (-D_i \nabla c_i) + \mathbf{u} \nabla c_i = R_i \quad (39)$$

where  $i = H_2, T_2$  and HT in gas phase, while  $i = H$  and T in solid phase, and  $\mathbf{u}$  denotes the velocity (m/s) in the gas phase.  $R_i$  is the source term for the corresponding component, e.g., isotopic exchange rate in gas phase.

The model domain includes the ARAA test sample, primary and secondary sides of the gas supply and return SS-316 tubing, and gold ring gasket as shown in Fig. 4.

The following modelling approach and solution methodology has been used:

1. The aforementioned H/T co-permeation model based on kinetic theory and the tritium isotope mass transport Eq. (39) has been implemented in COMSOL (Ref. 7).
2. Sieverts law conditions under a diffusion-controlled regime and/or surface-controlled boundary condition have been applied at gas/solid interface.

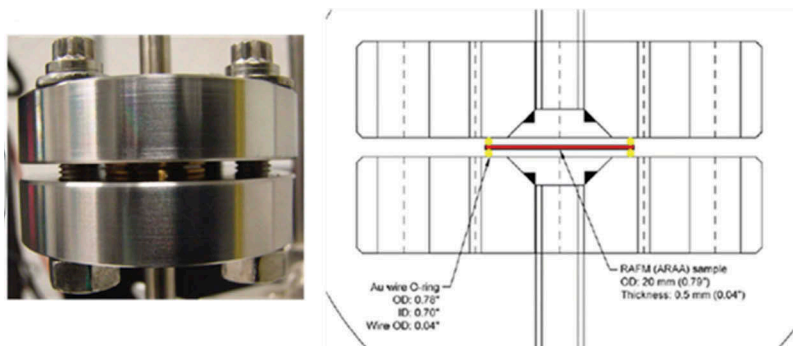


Fig. 3. Test section of tritium gas permeation from ARAA disk.

TABLE II  
Experimental Conditions

Material	ARAA
Dimension	20 mm OD, 0.5, 1.0, and 2.0 mm thickness
Temperature	400, 450, 500 °C
Primary gas	T <sub>2</sub> (10 <sup>-3</sup> ~ 10 <sup>-1</sup> Pa), H <sub>2</sub> (99Pa), and He at pressure of 10 <sup>5</sup> Pa; 50 sccm flow rate
Secondary gas	H <sub>2</sub> (99Pa), and He at pressure of 10 <sup>5</sup> Pa; 200 sccm flow rate

3. Isotope permeation is modeled by considering gas phase equilibriums between H<sub>2</sub>, T<sub>2</sub> and HT.

4. A scheme involving velocity-temperature-concentration coupling has been used.

The material properties used in the analysis are summarized in Table III.

#### IV. RESULTS AND DISCUSSIONS

Pre-analyses have been performed to help to define experimental design and operating conditions for tritium permeation experiments including: flow rate and gap distance, baking time, tube and ring materials, tube length, permeation time, etc. Figure 5 shows an example pre-analysis of tritium concentration (mol/m<sup>3</sup>) and gas flow in the test section. The operation conditions for this

Pre-analysis confirmed that the experimental conditions are appropriate for tritium permeation in the KO ARAA test. The calculation shows that tritium retained in the secondary SS pipe and gold O-ring is less than 0.1% of the permeated tritium throughout the ARAA sample. Meanwhile, the ion chamber is located at 6 feet downstream from the heated test section, which may cause tritium to be lost before it reaches the measuring point. However, the calculation shows that the temperature of the ion chamber pipes drops quickly from the test temperature to room temperature in about 0.3 m, which implies tritium loss after the furnace is low since the diffusivity and solubility are much lower at room temperature. The current design with a high flow rate (50–200 sccm) and a gap distance between inlet tube and sample of 1–1.6 mm results in good mixing. This in turn results in a uniform tritium pressure on the primary side of the ARAA surface. A baking time of 1800 s and a permeation time of 1800 s are calculated to be appropriate for the tritium permeation through KO ARAA test.

To validate the permeation model and to evaluate how different regimes affect the permeation amount, the permeation model was first validated by comparing with literature data of mono-isotope (deuterium) permeation through the RAFM material of MANET II under clean and oxidized samples. The material properties and experimental data are from E. Serra's work.<sup>6</sup> The experimental results for the bare and oxidized MANET II are obtained using discs of 48 mm in diameter and 0.5 mm in thickness. Before the membranes

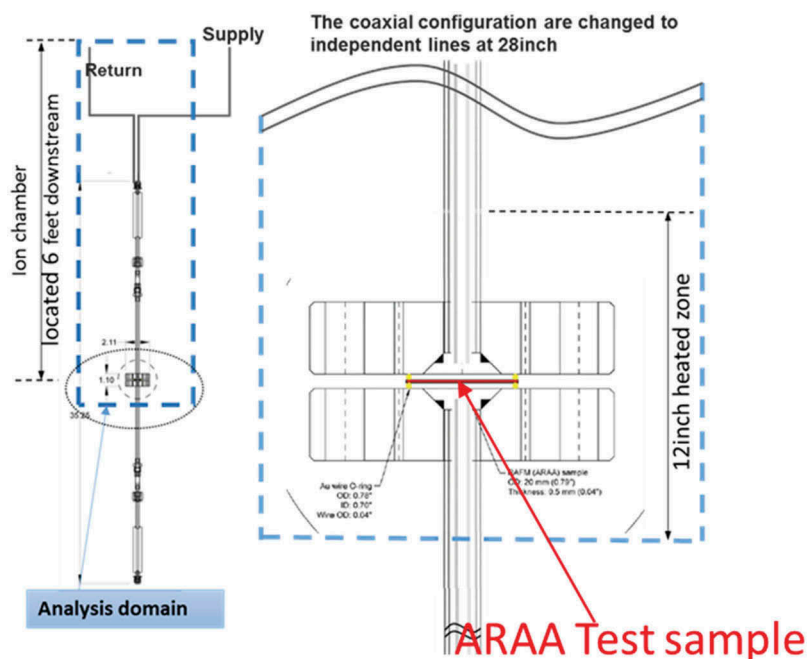


Fig. 4. Model calculation domain.

TABLE III  
The Material Properties Used in the Analysis

<b>SS-316 (H) (Ref. 8)</b>	
$K_s$	$1.11 \exp(-15713/RT) (\text{mol m}^{-3} \text{Pa}^{-0.5})$
$D$	$7.3 \times 10^{-7} \exp(-52378/RT) (\text{m}^2 \text{s}^{-1})$
<b>Gold (H) (Ref. 9)</b>	
$K_s$	$77.9 \exp(-99400/RT) (\text{mol m}^{-3} \text{Pa}^{-0.5})$
$D$	$5.6 \times 10^{-8} \exp(-99400/RT) (\text{m}^2 \text{s}^{-1})$
<b>F82H (D) (Ref. 7)</b>	
$K_s$	$0.37 \exp(-26880/RT) (\text{mol m}^{-3} \text{Pa}^{-0.5})$
$D$	$1.07 \times 10^{-7} \exp(-13950/RT) (\text{m}^2 \text{s}^{-1})$
<b>MANET II (D) (Ref. 5)</b>	
$K_s$	$0.27 \exp\left(-\frac{26670}{RT}\right) (\text{mol m}^{-3} \text{Pa}^{-0.5})$
$D$	$1.01 \times 10^{-7} \exp\left(-\frac{13210}{RT}\right) (\text{m}^2 \text{s}^{-1})$
<b>Bare MANET II (Ref. 5)</b>	
$\sigma k_1$	$5.56 \times 10^{-7} \exp\left(-\frac{19093}{RT}\right) (\text{mol m}^{-2} \text{s}^{-1} \text{Pa}^{-1})$
$\sigma k_2$	$7.63 \times 10^{-6} \exp\left(\frac{34247}{RT}\right) (\text{mol}^{-1} \text{m}^4 \text{s}^{-1})$
<b>Oxidized MANET II (Ref. 5)</b>	
$\sigma k_1$	$4.9 \times 10^{-7} \exp\left(-\frac{58383}{RT}\right) (\text{mol m}^{-2} \text{s}^{-1} \text{Pa}^{-1})$
$\sigma k_2$	$6.7 \times 10^{-6} \exp\left(-\frac{5044}{RT}\right) (\text{mol}^{-1} \text{m}^4 \text{s}^{-1})$
<b>ARAA (Ref. 10)</b>	
$P$	$9.8 \times 10^{-8} \exp\left(-\frac{47800}{kT}\right) \left(\frac{\text{mol}}{\text{m} \cdot \text{s} \cdot \text{Pa}^{0.5}}\right)$

are inserted into the permeation measuring equipment, the bare sample is mechanically polished while the oxidized disc, after the heat treatment in order to produce the fully martensitic phase, has been heated for 72 h in an

environment consisting of  $10^5$  Pa of  $\text{H}_2$  with about 1000 ppm of  $\text{H}_2\text{O}$ . From the experimental data, E. Serra obtained the Arrhenius expressions for the hydrogen isotopes surface constants on bare and oxidized MANET II as

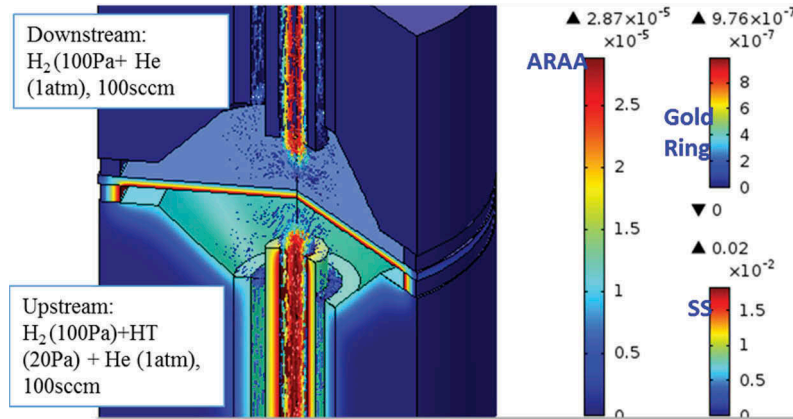


Fig. 5. Example tritium concentrations of pre-analysis.

listed in Table III. These surface constants representing different surface oxidation conditions along with a rate controlled boundary condition are applied in our simulations. Figure 6 shows the comparison of the steady state permeation flux vs. pressure for an oxidized MANET II sample and a bare MANET II sample. The scatter lines are experimental data and the colored symbols are simulation results. They agree very well for both oxidized and bare surfaces. The results indicated that 1) the permeation is surface-controlled for oxidized MANET II and it appears to be nearly first-order in  $p$  but becomes proportional to  $p^{1/2}$  for bare MANET II under a diffusion-controlled regime; 2) the permeation rate through oxidized sample is significantly reduced (~2 orders) compared with that of the clean sample.

A multi-component permeation validation was obtained by comparing the calculated permeation results with an initial set of experimental data obtained for a 0.5 mm thick KO ARAA clean sample at the INL TGAP facility. Figure 7 shows plotted tritium permeation flux versus temperature. Symbols are experimental data and lines are simulation results performed for conditions governed by surface-limited and diffusion-limited regimes. The simulations used tritium transport properties including diffusivity, solubility, desorption, and adsorption rate constants of MANET II (Ref. 6). It can be seen that for driving pressure of 0.048 Pa, the permeation fluxes given by the analytical Sieverts' law solutions (solid lines, no H<sub>2</sub> co-permeation effect, i.e. mono-isotope permeation) are much higher than the experimental data. If we consider the H/T co-permeation under diffusion-limited regime, the simulated tritium permeation flux agreed well with experimental data at high temperature, but over-predicted the data at low temperature. However, if we consider the H/T co-permeation under rate-limited condition using bare MANET surface properties, the agreement for tritium permeation flux was better at low temperature but under-predicted at high temperature. It seems to indicate that tritium behavior does not follow the square root of partial pressure dependence for diffusion-limited permeation.

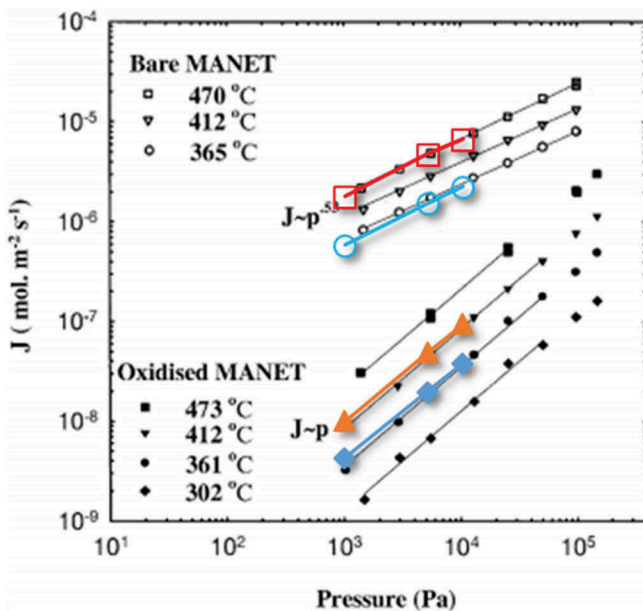


Fig. 6. Permeation rate of deuterium through oxidized and bare MANET II versus pressure.

It is worth noting that the initial tritium permeation campaign was carried out with pre-mixed tritium-helium gas. The H partial pressure was unknown in the initial permeation test, so T<sub>2</sub> partial pressure provided by the ion chamber is not accurate. A second tritium permeation campaign was carried out and the validations are described below.

The second tritium permeation campaign was then performed with a 0.5 mm thick KO ARAA clean sample with tritium-hydrogen (1000 ppm)-helium gas from the new tritium supply system (TSS). TSS is capable of changing tritium partial pressure by a factor of 20 while keeping hydrogen and helium concentration constant. Figure 8

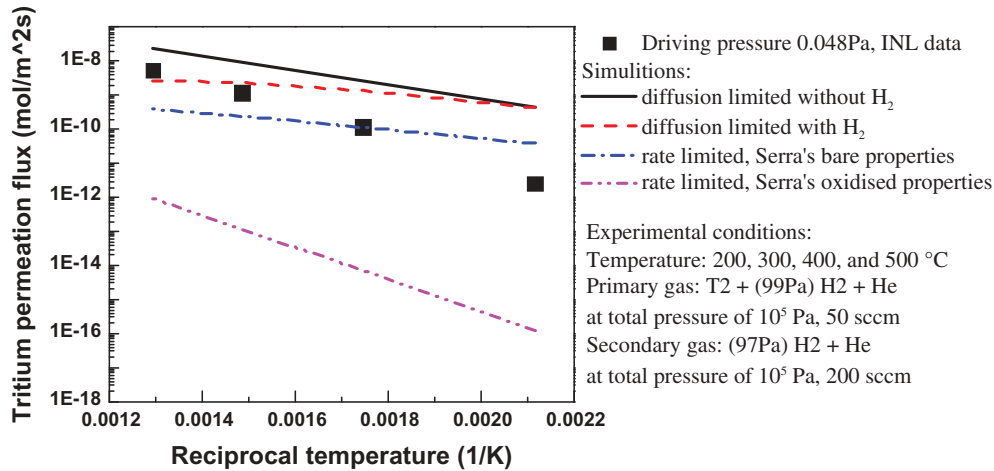


Fig. 7. Model simulations of an initial set of experimental data obtained at INL TGAP facility.

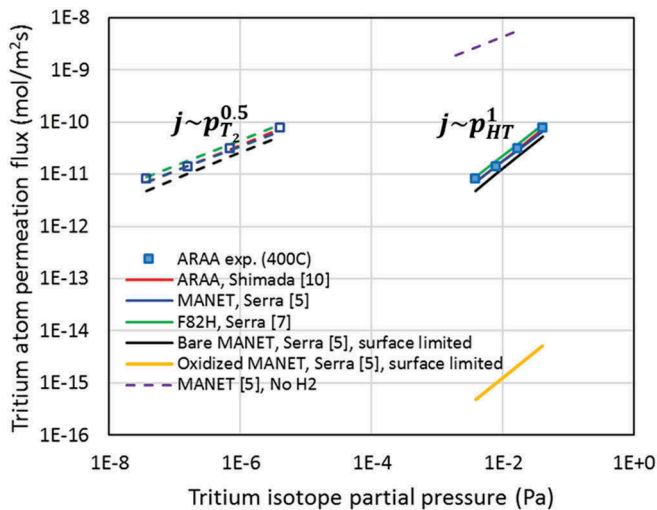


Fig. 8. Tritium permeation flux dependence on tritium isotope partial pressure of ARAA samples with tritium- (1000 ppm) hydrogen-helium gas.

shows the model simulations of the tritium permeation flux dependence on tritium isotope partial pressure of ARAA samples at 400°C. Symbols are experimental data obtained at the INL TGAP facility and lines are simulation results. Solid symbols and lines are permeation fluxes against HT partial pressure while open symbols and dashed lines are permeation fluxes against equilibrium T<sub>2</sub> partial pressure, where T<sub>2</sub> is calculated from equilibrium Eq. (32). Simulated results from reference material properties of F82H (Ref. 8), MANET II and MANET II bare and oxidized surfaces<sup>6</sup> were plotted for a comparison. The simulated tritium permeation fluxes agree well with experimental ARAA data with a diffusion-controlled mechanism. Predicted results using MANET II properties are also close to the experimental data while F82H

properties slightly over-predict the tritium permeation fluxes. However, the MANET II bare surface properties lead to under-prediction of the permeation fluxes with a surface-controlled mechanism. Both experimental data and simulation results seem to indicate that tritium permeation flux follows a diffusion-controlled, square root dependence of equilibrium T<sub>2</sub> partial pressure. Meanwhile, it also follows a linear dependence of HT partial pressure even though it is diffusion-limited permeation as stated in the equilibrium theory in Sec. II. In addition, both numerical simulations and experimental data confirm that the presence of hydrogen reduces the tritium permeation rate significantly in low tritium partial pressure with 1000 ppm (0.1%) hydrogen-helium gas mixture at 1atm.

## V. CONCLUSIONS

A kinetic model of co-permeation of H and T in a multi-component (H<sub>2</sub>, T<sub>2</sub> and HT) system was theoretically described. Under equilibrium condition, tritium equilibrium concentration on a metal surface follows a square root dependence of equilibrium T<sub>2</sub> partial pressure. Meanwhile, tritium concentration at equilibrium is also linearly dependent on HT partial pressure and inversely proportional to the square root of the partial pressure of H<sub>2</sub>. In addition, tritium permeation flux is significantly reduced by the presence of high pressure hydrogen. The model was validated by comparing the calculated results using several RAFM material properties (ARAA, F82H, MANET II) with INL ARAA experimental data at low tritium partial pressure of 0.001–0.1 Pa with a high hydrogen partial pressure of 100 Pa. The modeled tritium permeation fluxes using a diffusion-controlled mechanism agree well with experimental data, while it under-predicts

using a surface-controlled mechanism. Experimental behavior of tritium permeation flux dependence on tritium isotope partial pressure confirms the multi-components permeation model. The permeation model was also validated under a surface-controlled regime by comparing with literature data for MANET II under oxidized samples.

## Acknowledgments

This work was supported by the U. S. Department of Energy Contract DE-FG03-ER52123 and by the Task Agreement between UCLA-NFRI-INL for Cooperation on R&D for Fusion Nuclear Science to Expedite the Realization of Magnetic Fusion Energy.

## ORCID

Hongjie Zhang  <http://orcid.org/0000-0002-6590-7055>

## References

1. A. YING et al., “Advancement in Tritium Transport Simulations for Solid Breeding Blanket System,” *Fusion Eng. Des.*, **109–111**, 1511 (2016); <https://doi.org/10.1016/j.fusengdes.2015.11.040>.
2. D. W. LEE et al., “Integrated Design and Performance Analysis of the KO HCCR TBM for ITER,” *Fusion Eng. Des.*, **98–99**, 1821 (2015); <https://doi.org/10.1016/j.fusengdes.2015.06.141>.
3. G. A. ESTEBAN et al., “Hydrogen Isotope Diffusive Transport Parameters in Pure Polycrystalline Tungsten,” *J. Nucl. Mater.*, **295**, 49 (2001); [https://doi.org/10.1016/S0022-3115\(01\)00486-X](https://doi.org/10.1016/S0022-3115(01)00486-X).
4. K. KIZU, A. PISAREV, and T. TANABE, “Co-Permeation of Deuterium and Hydrogen Through Pd,” *J. Nucl. Mater.*, **289**, 291 (2001); [https://doi.org/10.1016/S0022-3115\(01\)00428-7](https://doi.org/10.1016/S0022-3115(01)00428-7).
5. R. LÄSSER and G. L. POWELL, “Solubility of Protium, Deuterium and Tritium in Palladium Silver Alloys at Low Hydrogen Concentrations,” *J. Less-Common Met.*, **130**, 387 (1987); [https://doi.org/10.1016/0022-5088\(87\)90133-0](https://doi.org/10.1016/0022-5088(87)90133-0).
6. E. SERRA, “Hydrogen and Tritium Kinetics in Fusion Reactor Materials,” Report EUR 16471 EN (1996).
7. *COMSOL Multiphysics User’s Guide*, v.5, COMSOL, Inc., Burlington, Massachusetts (2014).
8. E. SERRA, A. PERUJO, and G. BENAMATI, “Influence of Traps on the Deuterium Behaviour in the Low Activation Martensitic Steels F82H and Batman,” *J. Nucl. Mater.*, **245**, 108 (1997); [https://doi.org/10.1016/S0022-3115\(97\)00021-4](https://doi.org/10.1016/S0022-3115(97)00021-4).
9. D. M. GRANT, D. L. CUMMINGS, and D. A. BLACKBURN, “Hydrogen in 316 Steel- Diffusion, Permeation and Surface Reaction,” *J. Nucl. Mater.*, **152**, 139 (1988); [https://doi.org/10.1016/0022-3115\(88\)90319-4](https://doi.org/10.1016/0022-3115(88)90319-4).
10. R. CAUSEY, R. KARNESKY, and C. S. MARCHI, “Tritium Barrier and Tritium Diffusion in Fusion Reactors,” P.49, W. EICHENAUER and D. LIEBSCHER, “Measurement of the Diffusion Rate of Hydrogen in Gold,” *Z. Naturforsch.*, **17A**, 355 (1962).
11. A. YING et al., “Progress Report on Task Agreement Between the National Fusion Research Institute and the Regents of the University of California, Los Angeles for Cooperation on R&D for Fusion Nuclear Science to Expedite the Realization of Magnetic Fusion Energy” (July 2016).